

Chapter 7

Motion Detection for Reflexive Tracking

Frederick A. Miles and Boris M. Sheliga

Abstract The moving observer who looks in the direction of heading experiences radial optic flow, which is known to elicit horizontal vergence eye movements at short latency, expansion causing convergence and contraction causing divergence: the Radial Flow Vergence Response (RFVR). The moving observer who looks off to one side experiences linear flow, which is known to elicit horizontal version eye movements at short latency: the Ocular Following Response (OFR). Although the RFVR and OFR are very different kinds of eye movement and are sensitive to very different patterns of global motion, they have very similar local spatiotemporal properties. For example, both responses are critically dependent on the Fourier composition of the motion stimuli, consistent with early spatio-temporal filtering prior to motion detection, as in the well-known energy model of motion analysis. When the motion stimuli are sine-wave gratings, the two responses share a very similar dependence on the spatial frequency and contrast of those gratings, and even the quantitative details are very similar. When the motion consists of a single step (“two-frame movie”) then a brief inter-stimulus interval results in the reversal of both responses, consistent with the idea that both are mediated by motion detectors that receive a visual input whose temporal impulse response function is strongly biphasic. Further, when confronted with two sine-wave gratings that differ slightly in spatial frequency and have competing motions, both responses show nonlinear dependence on the relative contrasts of those two gratings: when the two sine waves differ in contrast by more than about an octave then the one with the higher contrast completely dominates the responses and the one with lower contrast loses its influence: winner-take-all. It has been suggested that these nonlinear interactions result from mutual inhibition between the low-level mechanisms sensing the motion of the different competing harmonics. Lastly, single unit recordings and local lesions in monkeys strongly suggest that both types of eye movements are

F.A. Miles (✉)

Laboratory of Sensorimotor Research, National Eye Institute/NIH,
Bldg 49 Rm 2A50, Bethesda, MD, 20892, USA
e-mail: fam@lsr.nei.nih.gov

mediated by neurons in the MT/MST region of the cerebral cortex that are sensitive to global optic flow. We will argue that these various findings are all consistent with the idea that the RFVR and OFR acquire their different global properties at the level of MT/MST, where the neurons respond to large-field radial and linear optic flow, and their shared local properties from a common earlier stage, the striate cortex, where the neurons respond to the local motion energy.

7.1 Two Different Kinds of Reflexive Eye Movement That Use Visual Motion

This chapter is concerned with two kinds of eye movements that are elicited at short latencies by large-field visual motion and function to help stabilize the gaze of the moving observer. The global structure of the visual motion conforms to the patterns of optic flow experienced by the moving observer who undergoes pure translation and determines which kind of eye movement is elicited. The overall pattern of the optic flow experienced during translation consists of radial streams of images emerging from a focus of expansion straight ahead and disappearing into a focus of contraction behind, cf., the lines of longitude on a globe. The *direction* of flow at any given point depends solely on the motion of the observer but the *speed* of the flow also depends on the 3-D structure of the visual surroundings, being inversely proportional to the viewing distance at that location. Thus, nearby objects move across the field of view much more rapidly than more distant ones: motion parallax (Gibson 1950, 1966). However, given the eyes' restricted fields of view, the pattern of motion actually seen depends on where the eyes are pointing relative to the direction of heading.

The moving observer who looks in the direction of heading sees a radially expanding pattern of flow and, as objects that lie ahead get closer, he/she converges his/her two eyes in order to keep the two foveas aligned on those objects utilizing a number of depth-tracking mechanisms. The mechanism of interest here is the so-called *Radial-Flow Vergence Response* (RFVR), which senses the radial flow and generates vergence (disconjugate) eye movements at ultra-short latency, <60 ms in monkeys and <80 ms in humans (Busetini et al. 1997; Inoue et al. 1998; Kodaka et al. 2007; Yang et al. 1999). When radial optic flow is applied to large random dot patterns, expansion causes convergence – consistent with compensation for forward motion of the observer – and contraction causes divergence – consistent with compensation for backward motion of the observer.

The moving observer who looks off to one side sees a laminar pattern of optic flow and, as nearby objects pass by, he/she tracks them with both eyes utilizing a number of conjugate tracking mechanisms. The one of interest here is the so-called *Ocular Following Response* (OFR), which senses the laminar flow and generates version (conjugate) eye movements at ultra-short latency (Barthélemy et al. 2006; Busetini et al. 1991; Masson and Castet 2002; Masson et al. 2000, 2001, 2002a, b; Miles and Kawano 1986; Miles et al. 1986a, b).

Clearly, these two oculomotor reflexes – the RFVR and the OFR – respond to very different kinds of global optic flow – radial and laminar – and generate two very different kinds of eye movement – *vergence* that alters the angle between the two lines of sight and thereby changes the distance to the plane of fixation, and *version* that alters the eccentricity of the two eyes together and thereby shifts gaze within the plane of fixation. Vergence (Vg), which is given by the difference in the positions of the two eyes $[L - R]$, and version (Vs), which is given by the average position of the two eyes $[(L + R)/2]$, are orthogonal representations and provide a complete description of binocular eye movements, so that the positions of each eye can be reconstructed from them. Thus, adopting the convention that rightward movement is positive, increases in convergence are also positive, and $L = Vs + Vg/2$ while $R = Vs - Vg/2$.

Although the RFVR and OFR utilize very different global patterns of optic flow (see Miles et al. 2004, for recent review), this chapter will concentrate on the properties of the local-motion detectors mediating these two reflexes, which we will argue are very similar, perhaps even the same. One important feature of all the experiments that will be reviewed is that they describe only the *initial open-loop eye movements*, that is, the eye movements generated within two reaction times. The reason for this is that the eye movements during this time are the direct result of the visual processing that occurred prior to response onset. Our general thesis is that these initial eye movements provide a powerful probe for investigating the early cortical processing of visual motion.

7.2 Responses to First-Order Motion Energy

Recent studies manipulated the Fourier composition of the visual stimuli used to elicit the OFR and the RFVR (Kodaka et al. 2007; Sheliga et al. 2005a, b, 2006b), employing a variety of spatial patterns including a square wave lacking the fundamental, which is the so-called missing fundamental (*mf*) stimulus. As first pointed out by Adelson (1982), the *mf* stimulus has the special property that, when advanced in $1/4$ -wavelength steps, its harmonics all shift $1/4$ of their respective wavelengths, the $4n + 1$ harmonics (like the 5th, 9th, etc.) in the forward direction and the $4n - 1$ harmonics (like the 3rd, 7th, etc.) in the backward direction. Importantly, the amplitude of the i th harmonic of the *mf* stimulus is proportional to $1/i$, so that the major Fourier component is the 3rd harmonic. It has been known for some time that when *mf* stimuli in the form of 1-D grating patterns are moved in successive $1/4$ -wavelength steps, the direction of perceived motion is often opposite to the actual motion (Adelson 1982; Adelson and Bergen 1985; Baro and Levinson 1988; Brown and He 2000; Georgeson and Harris 1990; Georgeson and Shackleton 1989). It is generally argued that 1st-order-motion detectors are responsible for the perception here and that these detectors are not sensing the motion of the raw images (or their features) but rather the motion energy in a spatially filtered version of the images, so that the perceived motion depends critically on the harmonic composition

of the spatial stimulus and especially the principal Fourier component, the 3rd harmonic. Note that when the *mf* stimulus shifts $\frac{1}{4}$ of its (fundamental) wavelength, the 3rd harmonic shifts $\frac{3}{4}$ of its wavelength in the same (forward) direction. However, a $\frac{3}{4}$ -wavelength *forward* shift of a sine wave is exactly equivalent to a $\frac{1}{4}$ -wavelength *backward* shift and, because the brain gives greatest weight to the nearest-neighbor matches (spatial aliasing), the perceived motion is generally in the backward direction: see Fig. 7.1. On the other hand, subjects sometimes perceive motion in the correct direction and this is generally attributed to higher-order detectors sensitive to the motion of specific features in the image. These observations are consistent with many others indicating that there are (at least) two neural

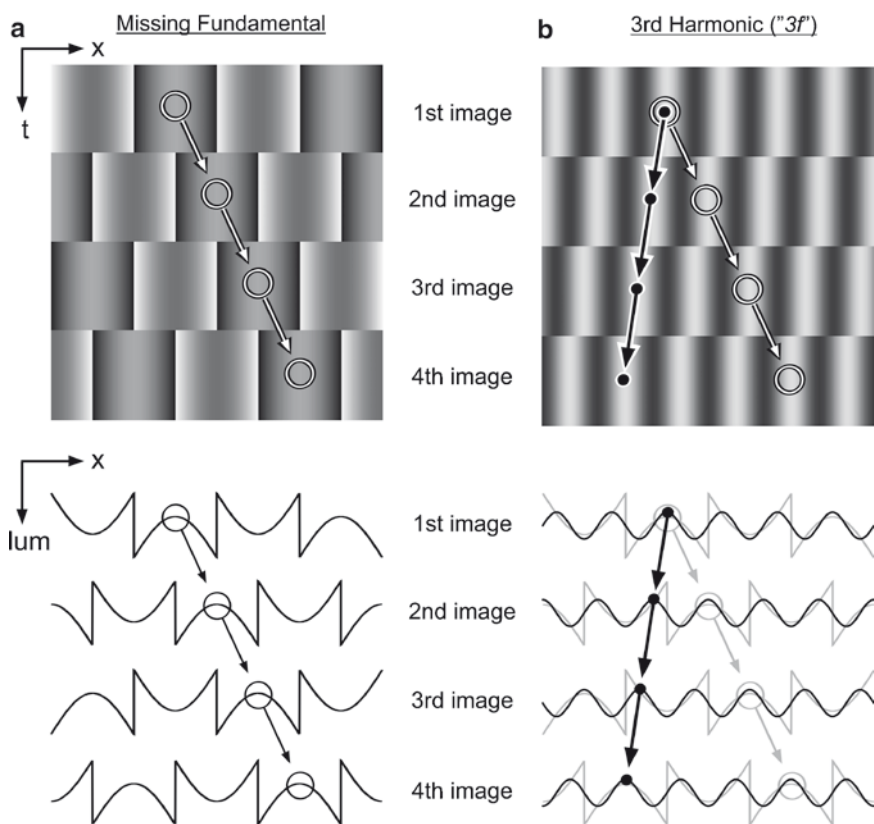


Fig. 7.1 The 1-D vertical *mf* stimulus grating and its 3rd harmonic. When the *mf* stimulus undergoes successive $\frac{1}{4}$ -wavelength steps to the right (**a**), its 3rd harmonic undergoes $\frac{3}{4}$ -wavelength steps to the right (**b**). *Upper panels* show horizontal slices through the stimuli at successive points in time (x - t plot) and *lower traces* show luminance as a function of horizontal spatial position (x - lum plot) after each step. The $\frac{3}{4}$ -wavelength rightward steps of the 3rd harmonic (gray circles linked by gray arrows in **b**) cannot be distinguished from $\frac{1}{4}$ -wavelength leftward steps (black dots linked by black arrows in **b**). In fact, when a pure sinusoid with the wavelength of the 3rd harmonic undergoes such steps it is invariably perceived to move leftwards, indicating that the brain gives greatest weight to the nearest matching images. After Chen et al. (2005), with permission (Wiley-Blackwell Publishing Ltd)

mechanisms by which we can sense visual motion.¹ The distinguishing characteristics of these mechanisms are sometimes controversial, and various descriptors have been applied to them: “short-range” vs. “long-range” (Braddick 1974), “1st-order” vs. “2nd-order” (Cavanagh and Mather 1989), “Fourier” vs. “non-Fourier” (Chubb and Sperling 1988), “passive” vs. “active” (Cavanagh 1992), and “energy-based” vs. “feature-based” or “correspondence-based” (Smith 1994).

Quarter-wavelength steps applied to 1-D *mf* grating stimuli elicit initial OFRs in the backward direction, i.e., in the direction of motion of the 3rd harmonic rather than the direction of motion of the overall pattern (Chen et al. 2005; Sheliga et al. 2005a). An example of such a response is shown in Fig. 7.2 (see trace labeled, *mf*).

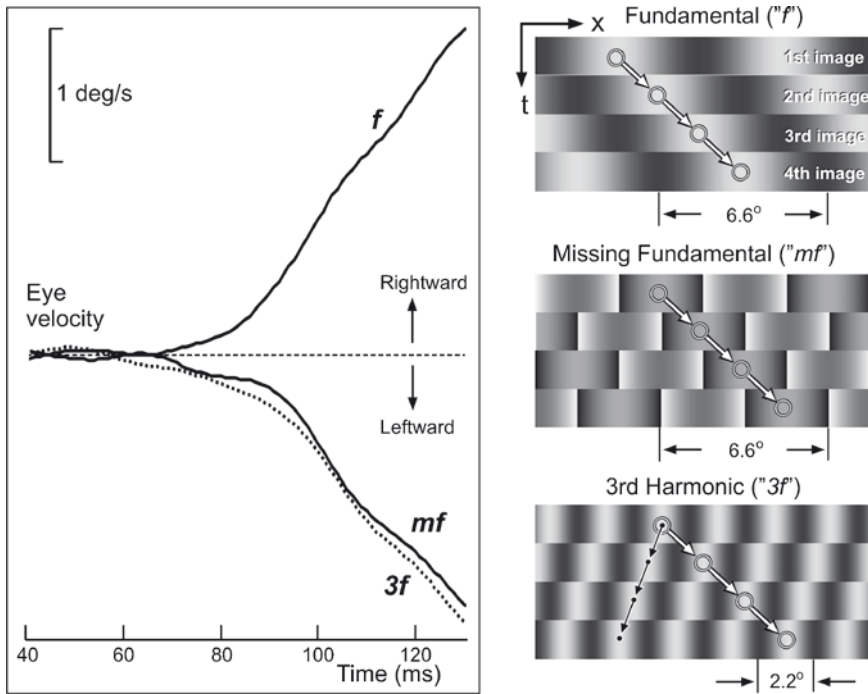


Fig. 7.2 The initial horizontal OFRs resulting from successive rightward steps applied to various 1-D vertical grating patterns (sample data for one subject). Trace *mf*: the initial OFR generated when the *mf* stimulus (wavelength, 6.6°) underwent successive ¼-wavelength rightward steps (1.65°). Trace *f*: the initial OFR when steps of the same magnitude (1.65°) and direction (rightward) were applied to pure sine-wave gratings that had the same spatial frequency as the fundamental (i.e., wavelength, 6.6°). Trace *3f*: the initial OFR when steps of the same magnitude (1.65°) and direction (rightward) were applied to pure sine-wave gratings that had the same spatial frequency and contrast (8%) as the principal Fourier component (3rd harmonic) of the *mf* stimulus. Note that time on the abscissa starts 40 ms after stimulus onset, and the *mf* and *3f* response profiles are almost identical. The cartoons at the right show *x-t* plots of the three stimuli, which all underwent the same motion steps (indicated by the circles and white arrows). After Chen et al. (2005), with permission (Wiley-Blackwell Publishing Ltd)

¹Lu and Sperling (1995, 1996, 2001) postulate *three* different mechanisms by which we sense motion.

It is important to note that when $\frac{1}{4}$ -wavelength steps are applied to 1-D gratings with a *pure sinusoidal* luminance profile the OFRs are always in the direction of those shifts (see f and $3f$ traces in Fig. 7.2), indicating that the motion detectors mediating the OFR give greatest weight to the nearest-neighbor matches. In fact, the OFRs to the mf stimuli were very similar to those when the same steps were applied to a pure sinusoid with the spatial frequency and contrast of the 3rd

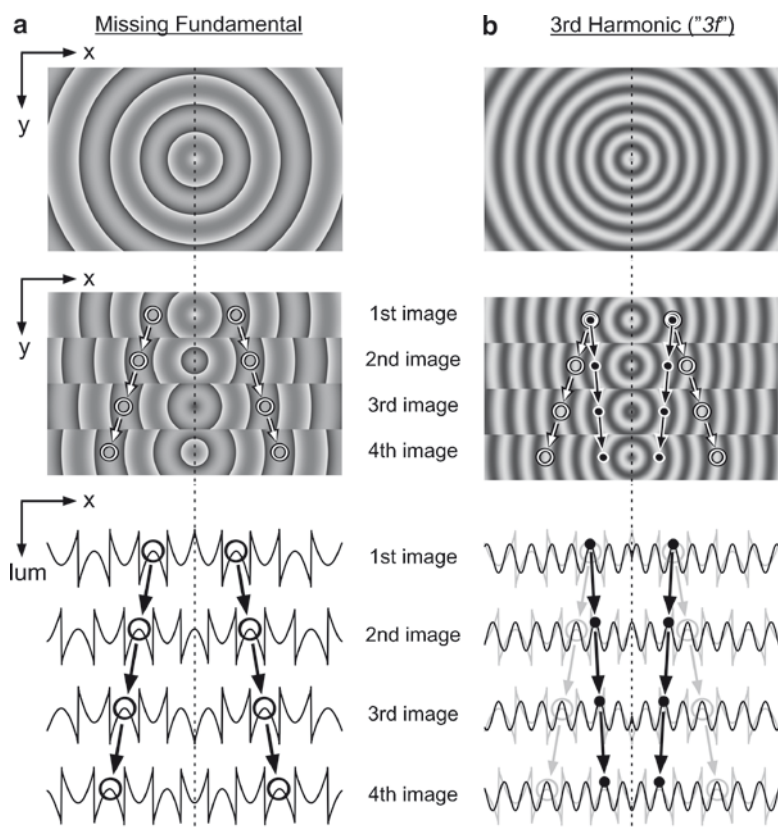


Fig. 7.3 The radial mf stimulus and its 3rd harmonic. When the mf stimulus undergoes successive $\frac{1}{4}$ -wavelength expansion steps (a), its 3rd harmonic undergoes $\frac{3}{4}$ -wavelength expansion steps (b). *Upper panels* show x - y luminance, indicating the appearance of the patterns on the screen at a given moment. *Middle panels* show horizontal slices through the centers of the x - y luminance plots after successive $\frac{1}{4}$ -wavelength expansions of the mf pattern. *Lower traces* show horizontal cross sections of the luminance profile through the center of the stimulus. The $\frac{3}{4}$ -wavelength expansion steps of the 3rd harmonic (gray circles linked by gray arrows in (b)) cannot be distinguished from $\frac{1}{4}$ -wavelength contraction steps (black dots linked by black arrows in (b)). In fact, when a concentric pattern with a sinusoidal radial luminance profile as in (b) undergoes such steps it is invariably perceived to contract, indicating that the brain gives greatest weight to the nearest matching images. Furthermore, the RFVRs elicited by stimuli like those in (a) and (b) are divergent (data not shown), consistent with contracting radial flow. After Kodaka et al. (2007)

harmonic: compare the mf and $3f$ traces in Fig. 7.2. These findings are consistent with the idea that the OFR is mediated by local-motion detectors sensitive to 1st-order motion, such as those in the well-known *energy model* of motion analysis (Adelson and Bergen 1985; van Santen and Sperling 1985; Watson and Ahumada 1985). Further support for this comes from the clear reversal of OFRs with “1st-order reverse-phi motion”, one of the hallmarks of an energy-based mechanism (Masson et al. 2002a).

In an analogous study on the RFVR (Kodaka et al. 2007), mf stimuli were arranged in concentric circles whose *radial* luminance modulation was that of a square wave with a missing fundamental and these patterns were subject to motion consisting of successive $\frac{1}{4}$ -wavelength *radial* steps: see Fig. 7.3. Once more it is important to note that when successive $\frac{1}{4}$ -wavelength radial shifts are applied to concentric patterns with a *pure sinusoidal* radial luminance profile the RFVRs conform to those seen with random-dot patterns – expansion steps cause convergence and contraction steps cause divergence – indicating that the local-motion detectors mediating the RFVR also give greatest weight to the nearest-neighbor matches. Analogous to the OFR, the RFVRs when $\frac{1}{4}$ -wavelength steps were applied to the radial mf stimulus were invariably reversed, so that expansion steps resulted in divergence and contraction steps resulted in convergence, and closely resembled the RFVRs elicited when the same radial steps were applied to concentric patterns with a pure sinusoidal luminance profile whose spatial frequency and contrast were the same as those of the 3rd harmonic (not shown). In sum, these data indicate that the local-motion detectors mediating both the OFR and the RFVR are sensitive to the 1st-order motion energy in the stimulus.

7.3 Non-Linear Interactions with Opponent Motion: Winner-Take-All (WTA)

Subsequent studies of the OFR that also used 1-D mf stimulus gratings examined the effect of *selectively* reducing the contrast of the principal Fourier component, the 3rd harmonic, while leaving the contrasts of the other harmonics unchanged (Sheliga et al. 2006c). This revealed the existence of powerful nonlinear interactions between the mechanisms sensing the various competing harmonics: as the contrast of the 3rd harmonic was reduced below that of the next most prominent harmonic, the 5th, then, as expected, the OFR reversed direction (because the 5th is a $4n+1$ harmonic whereas the 3rd is a $4n-1$ harmonic). However, surprisingly, once the contrast of that 3rd harmonic fell to less than $\frac{1}{2}$ the contrast of the 5th harmonic then further reductions in its contrast had no impact, as though the influence of that 3rd harmonic had been suppressed by the 5th harmonic, which was now the principal Fourier component and dominated the OFR. In the example data shown in Fig. 7.4a, the 5th harmonic of the mf stimulus had a contrast of 20%, and selectively reducing the contrast of the 3rd harmonic from 10 to 1% had almost no impact (closed circles in Fig. 7.4a), whereas the equivalent drop in the contrast

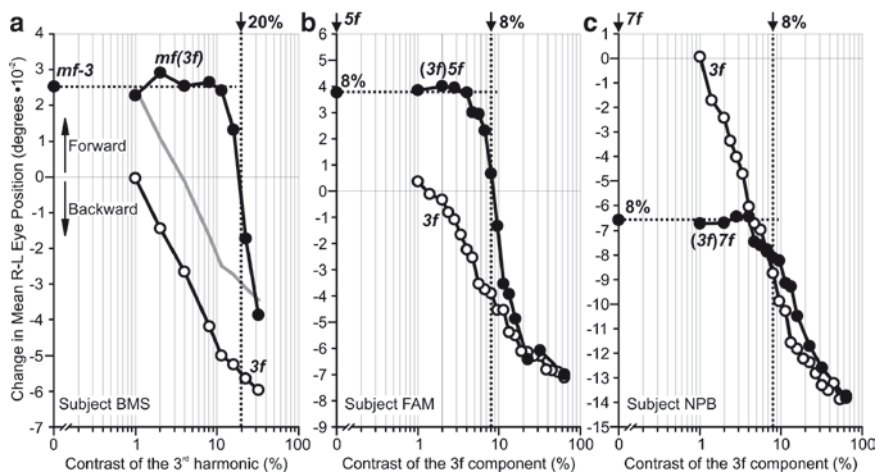


Fig. 7.4 Evidence for nonlinear interactions between the mechanisms sensing competing motions (sample response measures for one subject). (a) The initial OFRs to the *mf* stimuli: dependence on the contrast of the 3rd harmonic; plots show the OFR elicited by *mf* stimuli when the contrast of all other harmonics were held constant at the level they had when the 3rd harmonic was maximal, i.e., 32% (*closed circles*, labeled *mf(3f)*); plots also show the dependence on contrast of the OFRs to pure *3f* stimuli alone (*open circles*); the response to the *mf* stimulus that completely lacks the 3rd harmonic (*mf-3* stimulus) is plotted on the vertical axis (*filled circle* and extrapolated *horizontal dashed line*); also shown are the simulated OFRs based on the vector sum of the responses to the *mf-3* and *3f* stimuli (*gray continuous line*); the contrast of the 5th harmonic (20%) is indicated in vertical dotted line; the *mf(3f)* data are all plotted with respect to the contrast of the 3rd harmonic. (b) The initial OFRs to the competing *3f* and *5f* stimuli: dependence on the contrast of the *3f* component when the contrast of the *5f* component was fixed at 8% (*closed circles*, labeled *(3f)5f*); plots also show the OFR elicited by pure *3f* stimuli (*open circles*), and pure *5f* stimuli with 8% contrast (*closed circle* on the vertical axis and extrapolated *horizontal dashed line*); the *(3f)5f* data are all plotted with respect to the contrast of the *3f* component. (c) The initial OFRs to the competing *3f* and *7f* stimuli: dependence on the contrast of the *3f* component when the contrast of the *7f* component was fixed at 8% (*closed circles*, labeled *(3f)7f*); plots also show the OFR elicited by pure *3f* stimuli (*open circles*), and pure *7f* stimuli with 8% contrast (*closed circles* on the vertical axis and extrapolated *horizontal dashed line*). The *(3f)7f* data are all plotted with respect to the contrast of the *3f* component. Sample data from Sheliga et al. (2006c)

of a pure sinusoidal stimulus that had the same spatial frequency and underwent the same steps as that 3rd harmonic had a dramatic impact on the OFR (open circles labeled *3f* in Fig. 7.4a). This suggests that the neural channels carrying the information about the competing harmonics are mutually antagonistic so that if one harmonic has a contrast significantly greater than all others then it will tend to prevail over its competitors.

This idea was investigated further by restricting the moving stimuli to just two competing sine waves equivalent to the 3rd and 5th harmonics of the *mf* stimulus, so that their motions were in *opposite* directions. In the example data shown in Fig. 7.4b, the *5f* component always had a contrast of 8%, and increasing the

contrast of the $3f$ component from 1 to 4% had almost no impact (closed circles) whereas the equivalent increase in the contrast of the pure $3f$ stimulus alone had a dramatic impact on the OFR (open circles). Also, when the contrast of the $3f$ component was more than twice that of the $5f$ component (i.e., >16%) then the $5f$ component was now without influence and the responses now approximated those to the pure $3f$ stimulus alone. Systematically changing the contrast at which the $5f$ component was fixed indicated that the critical factor was the ratio of the contrasts of the competing gratings: when of similar contrast both were effective (vector sum/averaging), but when the contrast of one was less than about $\frac{1}{2}$ that of the other then the one with the higher contrast became dominant and the one with the lower contrast became ineffective: Winner-Take-All (WTA).

Analogous studies on the RFVR (Kodaka et al. 2007) used concentric circular patterns whose radial luminance modulation was that of two superimposed sine waves with spatial frequencies in the ratio 3:5. One grating underwent contracting steps and the other expanding steps, effectively mimicking the competing motions of the 3rd and 5th harmonics of the mf stimuli, and when the contrast of one exceeded that of the other, on an average, by a factor of almost two then the one with the higher contrast dominated the RFVRs and the one with lower contrast lost its influence (WTA).

This nonlinear behavior of the OFR and RFVR was attributed to mutual inhibition between the neural channels sensing the competing stimuli (cf., Ferrera 2000; Ferrera and Lisberger 1995, 1997; Recanzone and Wurtz 1999). One important issue is the spatial extent of these postulated inhibitory connections and this was recently investigated by recording the initial horizontal OFRs when horizontal motion in the form of successive $\frac{1}{4}$ -wavelength steps was applied in opposite directions to $3f$ and $5f$ 1-D vertical sine-wave gratings that were each confined to horizontal strips extending the full width of the display (45°) but only $1\text{--}2^\circ$ high (Sheliga et al. 2007a). The initial OFRs again showed strong dependence on the relative contrasts of the competing gratings and when these gratings were coextensive (i.e., overlapping) this dependence was always highly nonlinear, showing WTA behavior, exactly as with the full-screen overlapping gratings used in the previous OFR study. However, a vertical gap of 1° between the competing gratings was sufficient to completely eliminate the nonlinear interaction and OFRs now approximated the vector sum of the responses to each grating stimulus alone. Thus, the nonlinear interactions responsible for the WTA outcome were strictly local, indicating that the postulated inhibitory connections do not extend much beyond the confines of the visual stimuli.

The postulated mutual inhibition between channels subserving opposite directions of motion is often termed, “motion opponency”, and has substantial supporting evidence from psychophysical studies (Levinson and Sekuler 1975; Mather and Moulden 1983; Qian et al. 1994; Stromeyer et al. 1984; van Santen and Sperling 1984; Zeman et al. 1998), functional magnetic resonance imaging (Heeger et al. 1999), and single unit recordings in area MT (Bradley et al. 1995; Mikami et al. 1986; Qian and Andersen 1994; Rodman and Albright 1987; Rust 2004; Snowden et al. 1991) and area V1 (Rust 2004; Rust et al. 2005). Interestingly, Rust (2004) concluded that MT inherited motion opponency from V1.

From the functional viewpoint, it has been suggested that motion opponency will improve noise immunity and increase directional selectivity (Born and Bradley 2005; Qian et al. 1994). Also, in recent neuronal models of motion processing, motion opponency makes an important contribution to the *pattern selectivity* evident in some MT neurons (Rust et al. 2006). The study that demonstrated WTA behavior in the OFR (Sheliga et al. 2006c) argued that the strong preference given to the images with higher contrast would give objects in the plane of fixation an advantage: because of accommodation, the retinal images of objects in the plane of fixation will tend to be better focused – and hence tend to have higher contrasts – than those of objects in other depth planes. It was pointed out that this would be in line with earlier studies, which showed that when random-dot stimuli are used, the OFR is effectively disabled by binocular disparities of more than a few degrees (Masson et al. 2001; Yang et al. 2003; Yang and Miles 2003), suggesting that the motion detectors mediating the OFR are also disparity selective and that, in everyday conditions, these reflexes will have a strong preference for objects in the immediate vicinity of the plane of fixation and will tend to ignore objects in other depth planes. This same reasoning could be applied to the RFVR but, as pointed out by Kodaka et al. (2007), it is not clear how favoring images moving in the plane of fixation would necessarily operate to this system's advantage.

7.4 Non-Linear Interactions with Component Motion: WTA and Normalization

The OFR study of Sheliga et al. (2006c) that reported WTA behavior with opponent motion also included experiments with two competing 1-D sine waves that were equivalent to the 3rd and 7th harmonics of the *mf* stimulus so that their motions were in the *same* direction, here termed *component* motion. In the example data shown in Fig. 7.4c, the *7f* component always had a contrast of 8%, and increasing the contrast of the *3f* component from 1 to 4% had almost no impact (closed circles) whereas the equivalent increase in the contrast of the pure *3f* stimulus alone had a dramatic impact on the OFR (open circles). Also, when the contrast of the *3f* component exceeded twice that of the *7f* component (i.e., >16%) then the *7f* component was now without influence and the responses now approximated those to the *3f* stimulus alone. Systematically changing the contrast at which the *7f* component was fixed again indicated that the critical factor was the ratio of the contrasts of the competing gratings: when of similar contrast both were effective (vector sum/averaging), but when the contrast of one was less than about ½ that of the other then the one with the higher contrast became dominant and the one with the lower contrast became ineffective: Winner-Take-All (WTA). When the two gratings were each confined to horizontal strips only 1–2° high this nonlinear interaction was still very robust when the two gratings were overlapping (Sheliga et al. 2007a). However, unlike the situation with the *3f* and *5f* stimulus strips, separating the *3f* and *7f* grating strips by a vertical gap of up to 8° (the largest separation tried)

reduced the nonlinear interaction somewhat but did not eliminate it and OFRs were still far short of the linear sum of the responses to each grating alone. The suggestion here is that the inhibitory interactions generally postulated to account for the WTA behavior are again very local but there are also more global inhibitory interactions resembling the divisive normalization often described in visual-motion-sensitive neurons in the cortex (Britten and Heuer 1999; Carandini and Heeger 1994; Carandini et al. 1997; Heeger 1992; Heuer and Britten 2002; Simoncelli and Heeger 1998).

This postulated global normalization was recently examined further by recording the horizontal OFRs to successive $\frac{1}{4}$ -wavelength steps applied to a single 1-D vertical sine-wave grating that could occupy the full monitor screen (45° wide, 30° high) or a number of horizontal strips, each 1° high and extending the full width of the display (Sheliga et al. 2008). These strips were always equally spaced vertically, and increasing the number of strips could reduce the response latency by up to 20 ms, so the magnitude of the initial OFRs was estimated from the change in eye position over the initial open-loop period measured with respect to response onset. A single (centered) strip (covering 3.3% of the screen) always elicited robust OFRs, and 3 strips (10% coverage) were sufficient to elicit the maximum OFR. Further increasing the number of strips to 15 (50% coverage) had little impact, i.e., responses had asymptoted, and further increasing the coverage to 100% (full screen image) actually *decreased* the OFR so that it was now less than that elicited with only 1 strip. In this experiment, the gratings always had the same contrast, and in a second experiment, the contrast of the gratings could be fixed at one of four levels: the OFR showed essentially the same pattern of dependence on the number of strips (i.e., screen coverage) at any given contrast but, significantly, the lower the contrast, the lower the level at which the response asymptoted. This indicated that the asymptote was *not* due simply to the passive achievement of some intrinsic upper limit in the magnitude of the eye movement or the underlying motion signals (“ceiling effect”). Rather, this asymptote was seen as the result of an active process consistent with the normalization attributed to global divisive inhibition among cortical neurons cited in the previous paragraph.

Sheliga et al. (2008) attributed the *decrease* in the OFR when the image filled the monitor screen to the increased continuity of the gratings arguing that it would favor the local inhibitory surround mechanisms over the central excitatory ones (cf., Barthélemy et al. 2006). Direction-selective neurons with powerful inhibitory surrounds are commonplace in cortical area MT, which is a major source of the motion signals reaching MST, a region known to be critical for the genesis of the OFR (Takemura et al. 2007). Some MT neurons have antagonistic surrounds whose preferred direction of motion is the same as that at the center, rendering these neurons sensitive to local-motion contrast and insensitive to wide-field motion: see Born and Bradley (2005) for recent review. Sheliga et al. (2008) suggested that it is because of such neurons that introducing spatial discontinuities increases the OFR – even while decreasing the area stimulated by the motion – by reducing the activation of the antagonistic surrounds. This study indicates that robust OFRs can be elicited by much smaller motion stimuli

than are commonly used and strongly suggests that this is because of divisive normalization and inhibitory surround mechanisms. Ideally, the responses of an ocular tracking mechanism to motion of a given speed and direction should be insensitive to the physical characteristics of the moving images and these new data indicate that, for a given contrast, the initial OFRs are independent of the size of the stimulus over a five-fold range (10–50% coverage). Over this range, there is clear vector averaging, exactly the sort of behavior one expects of a system subject to divisive normalization. Sheliga et al. (2008) suggested that these effects are mediated by the same mechanism that is responsible for contrast gain control whereby the OFR saturates at relatively low contrast, ~30% (Masson and Castet 2002; Sheliga et al. 2005a).

A crucial feature of the study of Sheliga et al. (2008) was that the stimuli were in effect seen through elongated apertures aligned with the axis of motion and hence were inherently broadband. Moving images confined to stationary circular apertures, as in the study of Barthélemy et al. (2006), become increasingly high-pass when the aperture is reduced in diameter, compromising the low spatial frequencies that are preferred by the OFR. Thus, the effects of the aperture here are less to do with its area than with its spatial-frequency bandwidth, which depends on the length of the aperture along the axis of motion. Many other studies have examined the so-called smooth pursuit tracking responses to single small moving spots that are obviously not confined to a stationary window, but these pursuit responses have latencies that are generally at least twice that of the OFR (e.g., Heinen and Watamaniuk 1998).

7.5 Dynamics: The Biphasic Temporal Impulse Response

Recent studies using two-frame movies, i.e., single steps, to elicit OFRs and RFVRs showed that brief ISIs (10–100 ms) reversed the initial direction of these responses (Kodaka et al. 2007; Sheliga et al. 2006a). Sample data showing this effect for the OFR can be seen in Fig. 7.5a. These reversals are reminiscent of the oft-reported reversal of perceived motion by brief ISIs that has generally been attributed to the temporal dynamics of the early visual pathway and, in particular, to the negative phase of the well-known biphasic temporal impulse response function of the human visual system (Pantle and Turano 1992; Shioiri and Cavanagh 1990; Strout et al. 1994; Takeuchi and De Valois 1997; Takeuchi et al. 2001). In this scheme, the polarity of the visual responses reaching the underlying motion detectors is assumed to undergo reversal during the ISI, so that the neural representation of the 2nd image – whose appearance marks the onset of motion – is matched to a representation of the 1st image that has undergone (transient) reversal during the ISI. This 180° phase shift in the neural representation of the 1st image means that the $\frac{1}{4}$ -wavelength difference between the 1st and 2nd stimuli would be seen as a 90° phase shift in one direction when there is no ISI and as a 90° phase shift in the opposite direction when there is a brief ISI.

The consensus from the above-mentioned psychophysical studies was that with ISIs of less than ~100 ms the perceived motion depended on 1st-order energy-based

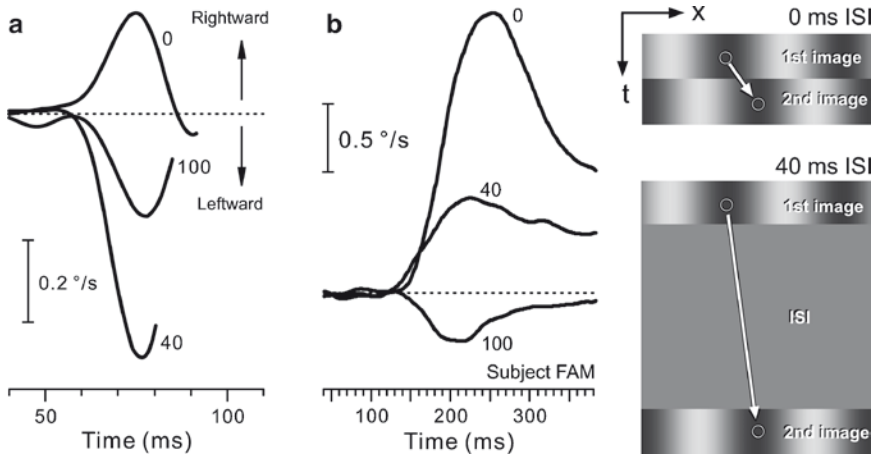


Fig. 7.5 The initial horizontal OFRs elicited by two-frame movies (single $\frac{1}{4}$ -wavelength rightward steps) applied to 1-D vertical gratings: dependence of mean eye velocity response profiles on an intervening luminance-matched period of gray, the ISI (one subject). **(a)** Photopic conditions. **(b)** Scotopic conditions. The ISIs, indicating the time interval between the disappearance of the 1st image and the appearance of the 2nd image, were 0, 40 or 100 ms (numbers on the traces). Note that time on the abscissa starts 40 ms after the appearance of the 2nd image. Upward deflections of the traces denote rightward eye movements. *Dotted lines* indicate zero eye velocity. Contrast was always 32%. Sample traces from Sheliga et al. (2006a). The cartoons at the right show $x-t$ plots of the stimuli when the ISI was 0 ms (above) and 40 ms (below)

mechanisms, whereas any perceived motion with longer ISIs depended on higher-order feature-based mechanisms. Thus, the reversal of the OFR and RFVR with short ISIs is a further support for mediation by detectors sensitive to 1st-order motion energy.

The dependence of the initial OFR on the ISI has also been shown to be very sensitive to the mean luminance level. Thus, the strong reversal of the initial OFR with ISIs of 10–60 ms seen in Fig. 7.5a was obtained under photopic conditions and the reversed OFRs actually reached much higher velocities than the non-reversed OFRs with 0-ms ISI. However, under scotopic conditions, reversal occurred only with ISIs ≥ 60 ms and these reversed OFRs were always appreciably weaker than the non-reversed OFRs with 0-ms ISI: see Fig. 7.5b, for which the luminance was below the human cone threshold. That the dependence of OFRs on the ISI shifted from biphasic to more monophasic with dark adaptation accords with the changes in the human modulation transfer function from band-pass to low-pass in the frequency domain and from biphasic to monophasic in the time domain (Kelly 1961, 1971a, b; Roufs 1972a, b; Snowden et al. 1995; Swanson et al. 1987). Note that the reversal of perceived motion with intermediate ISIs (30–90 ms) reported by Takeuchi and De Valois (1997) was obtained under photopic viewing conditions and these workers also showed that the reversal was reduced at low luminance. In fact, when the retinal illuminance was reduced below cone threshold, Takeuchi and De Valois (1997) found that ISIs no longer reversed perceived motion.

7.6 Neural Mediation

There is extensive evidence from monkeys that the OFR and RFVR are cortically mediated despite their ultra-short latency. Bilateral lesions of the medial superior temporal area of the cortex (MST) result in major impairments of both reflexes (Takemura et al. 2002, 2007) and there is extensive data from single unit recordings indicating that neurons in this region discharge in relation to the visual stimuli used to drive these reflexes. Thus, MST is specialized for the processing of optic flow (for recent review, see Wurtz 1998) and has long been known to contain neurons that are selectively sensitive to radial optic flow patterns such as those used to evoke RFVRs at ultra-short latencies (Duffy 2000; Duffy and Wurtz 1991a, b, 1995, 1997a, b, c; Lagae et al. 1994; Saito et al. 1986; Tanaka et al. 1986; Tanaka and Saito 1989). Kawano and colleagues have shown that there are neurons in MST that discharge in relation to the earliest OFR responses, their temporal profiles even reproducing the irregularities in the temporal profiles of the OFRs (Kawano et al. 1994; Takemura et al. 2000; Takemura and Kawano 2006). This cortical region is thought to rely heavily on magnocellular pathways, which are so named because they include the magnocellular layers of the LGN (Livingstone and Hubel 1987, 1988; Maunsell et al. 1990; Merigan and Maunsell 1990; Schiller et al. 1990). The contrast-dependence of the OFR in monkeys (Miles et al. 1986a) and humans (Masson and Castet 2002; Sheliga et al. 2005a), and of the RFVR in humans (Kodaka et al. 2007), closely resemble that in the magnocellular pathway, which is characterized by saturation at relatively low contrast levels (Kaplan and Shapley 1982). Recordings from monkeys also indicate that, at scotopic luminance levels, vision is dominated by rod inputs to magnocellular-projecting retinal ganglion cells (Lee et al. 1997; Purpura et al. 1988), consistent with the finding of Sheliga et al. (2006a) that the OFR continues to operate even at very low luminance and contrast levels. Lesions and electrophysiological studies in monkeys strongly suggest that the OFR is mediated by projections from MST to the dorsolateral pons, which then projects to the ventral paraflocculus, a region of the cerebellum well known for its involvement with the generation of tracking eye movements (see Takemura and Kawano 2002, for review).

7.7 A Window onto the Processing of Visual Motion in the Human Striate Cortex?

Earlier studies suggested that the OFR and RFVR are synergistic reflexes² that combine to assist in the visual stabilization of the gaze of the moving observer and pointed out a number of shared features in addition to their ultra-short latency, such

²We have not mentioned a 3rd reflex, the Disparity Vergence Response, that is also thought to be a member of this family, because it responds to binocular disparity rather than motion. This reflex shares many fundamental properties with the OFR and RFVR, including dependence on 1st-order (disparity) energy (Sheliga et al. 2006b), and WTA behavior when competing (disparity) stimuli are used (Sheliga et al. 2007b).

as post-saccadic enhancement, dependence on the preëxisting vergence angle, and – in monkeys at least – mediation by MST: for review see Miles (1998), Miles et al. (2004) and Takemura et al. (2007). More recently, Kodaka et al. (2007) showed that the fundamental spatiotemporal characteristics of the OFR and RFVR – such as their dependence on contrast, spatial frequency and an ISI, as well as the nonlinear interactions that are evident with competing motions – were very similar, quantitatively as well as qualitatively. Kodaka et al. (2007) suggested that these two very different kinds of eye movements share these basic spatiotemporal properties because they are mediated by the same low-level, local-motion detectors. As pointed out above, work on monkeys strongly implicates the MST area of cortex in the genesis of the RFVR and OFR, and this area is known to receive major inputs from area MT (Maunsell and van Essen 1983; Ungerleider and Desimone 1986), which receives a direct projection from direction-selective neurons in V1 (Movshon and Newsome 1996). Of particular interest is that recent authors have suggested that neurons in MT inherit their local-motion selectivity from neurons in V1 (e.g., Born and Bradley 2005; Churchland et al. 2005; Movshon and Newsome 1996; Priebe et al. 2006; Rust 2004; Rust et al. 2006). This raises the possibility that the local spatiotemporal properties of the MST neurons mediating both the RFVR and the OFR directly reflect the local motion energy computed by V1 direction-selective neurons. Thus, even though the MST neurons mediating these two reflexes must have very different global properties – preferring radial vs. linear optic flow, respectively – they nonetheless probably share the same local spatiotemporal characteristics. One especially attractive feature of these two reflexes is that many of their basic characteristics are well captured by simple mathematical functions with only two free parameters (e.g., dependence on log spatial frequency is Gaussian, dependence on contrast is well described by the Naka–Rushton equation, and dependence on the relative contrast of two competing motions is well described by a Contrast-Weighted-Average model) and these quantitative characterizations generally show little inter-subject variability. Thus, although the OFR and RFVR are *motor* responses, they directly reflect the detailed properties of the low-level *sensory* detectors mediating those responses and effectively provide a quantitative window onto the early cortical processing of visual motion, perhaps as early as striate cortex.

Acknowledgments This research was supported by the Intramural Research Program of the National Eye Institute at the NIH.

References

- Adelson EH (1982). Some new motion illusions, and some old ones, analysed in terms of their Fourier components. *Invest Ophthalmol Vis Sci*, 34 (Suppl.):144 (Abstract)
- Adelson EH, Bergen JR (1985) Spatiotemporal energy models for the perception of motion. *J Opt Soc Am A* 2:284–299
- Baro JA, Levinson E (1988) Apparent motion can be perceived between patterns with dissimilar spatial frequencies. *Vision Res* 28:1311–1313

- Barthélemy FV, Vanzetta I, Masson GS (2006) Behavioral receptive field for ocular following in humans: dynamics of spatial summation and center-surround interactions. *J Neurophysiol* 95:3712–3726
- Born RT, Bradley DC (2005) Structure and function of visual area MT. *Annu Rev Neurosci* 28:157–189
- Braddick O (1974) A short-range process in apparent motion. *Vision Res* 14:519–527
- Bradley DC, Qian N, Andersen RA (1995) Integration of motion and stereopsis in middle temporal cortical area of macaques. *Nature* 373:609–611
- Britten KH, Heuer HW (1999) Spatial summation in the receptive fields of MT neurons. *J Neurosci* 19:5074–5084
- Brown RO, He S (2000) Visual motion of missing-fundamental patterns: motion energy versus feature correspondence. *Vision Res* 40:2135–2147
- Busetтини C, Masson GS, Miles FA (1997) Radial optic flow induces vergence eye movements with ultra-short latencies. *Nature* 390:512–515
- Busetтини C, Miles FA, Schwarz U (1991) Ocular responses to translation and their dependence on viewing distance. II. Motion of the scene. *J Neurophysiol* 66:865–878
- Carandini M, Heeger DJ (1994) Summation and division by neurons in primate visual cortex. *Science* 264:1333–1336
- Carandini M, Heeger DJ, Movshon JA (1997) Linearity and normalization in simple cells of the macaque primary visual cortex. *J Neurosci* 17:8621–8644
- Cavanagh P (1992) Attention-based motion perception. *Science* 257:1563–1565
- Cavanagh P, Mather G (1989) Motion: the long and short of it. *Spat Vis* 4:103–129
- Chen KJ, Sheliga BM, FitzGibbon EJ, Miles FA (2005) Initial ocular following in humans depends critically on the fourier components of the motion stimulus. *Ann N Y Acad Sci* 1039:260–271
- Chubb C, Sperling G (1988) Drift-balanced random stimuli: a general basis for studying non-Fourier motion perception. *J Opt Soc Am A* 5:1986–2007
- Churchland MM, Priebe NJ, Lisberger SG (2005) Comparison of the spatial limits on direction selectivity in visual areas MT and V1. *J Neurophysiol* 93:1235–1245
- Duffy CJ (2000) Optic flow analysis for self-movement perception. *Int Rev Neurobiol* 44:199–218
- Duffy CJ, Wurtz RH (1991a) Sensitivity of MST neurons to optic flow stimuli. I. A continuum of response selectivity to large-field stimuli. *J Neurophysiol* 65:1329–1345
- Duffy CJ, Wurtz RH (1991b) Sensitivity of MST neurons to optic flow stimuli. II. Mechanisms of response selectivity revealed by small-field stimuli. *J Neurophysiol* 65:1346–1359
- Duffy CJ, Wurtz RH (1995) Response of monkey MST neurons to optic flow stimuli with shifted centers of motion. *J Neurosci* 15:5192–5208
- Duffy CJ, Wurtz RH (1997a) Medial superior temporal area neurons respond to speed patterns in optic flow. *J Neurosci* 17:2839–2851
- Duffy CJ, Wurtz RH (1997b) Multiple temporal components of optic flow responses in MST neurons. *Exp Brain Res* 114:472–482
- Duffy CJ, Wurtz RH (1997c) Planar directional contributions to optic flow responses in MST neurons. *J Neurophysiol* 77:782–796
- Ferrera VP (2000) Task-dependent modulation of the sensorimotor transformation for smooth pursuit eye movements. *J Neurophysiol* 84:2725–2738
- Ferrera VP, Lisberger SG (1995) Attention and target selection for smooth pursuit eye movements. *J Neurosci* 15:7472–7484
- Ferrera VP, Lisberger SG (1997) The effect of a moving distractor on the initiation of smooth-pursuit eye movements. *Vis Neurosci* 14:323–338
- Georgeson MA, Harris MG (1990) The temporal range of motion sensing and motion perception. *Vision Res* 30:615–619
- Georgeson MA, Shackleton TM (1989) Monocular motion sensing, binocular motion perception. *Vision Res* 29:1511–1523
- Gibson JJ (1950) *The perception of the visual world*. Houghton Mifflin, Boston
- Gibson JJ (1966) *The senses considered as perceptual systems*. Houghton Mifflin, Boston

- Heeger DJ (1992) Normalization of cell responses in cat striate cortex. *Vis Neurosci* 9:181–197
- Heeger DJ, Boynton GM, Demb JB, Seidemann E, Newsome WT (1999) Motion opponency in visual cortex. *J Neurosci* 19:7162–7174
- Heinen SJ, Watamaniuk SN (1998) Spatial integration in human smooth pursuit. *Vision Res* 38:3785–3794
- Heuer HW, Britten KH (2002) Contrast dependence of response normalization in area MT of the rhesus macaque. *J Neurophysiol* 88:3398–3408
- Inoue Y, Takemura A, Suehiro K, Kodaka Y, Kawano K (1998) Short-latency vergence eye movements elicited by looming step in monkeys. *Neurosci Res* 32:185–188
- Kaplan E, Shapley RM (1982) X and Y cells in the lateral geniculate nucleus of macaque monkeys. *J Physiol (Lond)* 330:125–143
- Kawano K, Shidara M, Watanabe Y, Yamane S (1994) Neural activity in cortical area MST of alert monkey during ocular following responses. *J Neurophysiol* 71:2305–2324
- Kelly DH (1961) Visual response to time-dependent stimuli. I. Amplitude sensitivity measurements. *J Opt Soc Am* 51:422–429
- Kelly DH (1971a) Theory of flicker and transient responses. I. Uniform fields. *J Opt Soc Am* 61:537–546
- Kelly DH (1971b) Theory of flicker and transient responses. II. Counterphase gratings. *J Opt Soc Am* 61:632–640
- Kodaka Y, Sheliga BM, Fitzgibbon EJ, Miles FA (2007) The vergence eye movements induced by radial optic flow: some fundamental properties of the underlying local-motion detectors. *Vision Res* 47:2637–2660
- Lagae L, Maes H, Raiguel S, Xiao D-K, Orban GA (1994) Responses of macaque STS neurons to optic flow components: a comparison of areas MT and MST. *J Neurophysiol* 71:1597–1626
- Lee BB, Smith VC, Pokorny J, Kremers J (1997) Rod inputs to macaque ganglion cells. *Vision Res* 37:2813–2828
- Levinson E, Sekuler R (1975) Inhibition and disinhibition of direction-specific mechanisms in human vision. *Nature* 254:692–694
- Livingstone M, Hubel DH (1988) Segregation of form, color, movement, and depth: anatomy, physiology, and perception. *Science* 240:740–749
- Livingstone MS, Hubel DH (1987) Psychophysical evidence for separate channels for the perception of form, color, movement, and depth. *J Neurosci* 7:3416–3468
- Lu ZL, Sperling G (1995) The functional architecture of human visual motion perception. *Vision Res* 35:2697–2722
- Lu ZL, Sperling G (1996) Three systems for visual motion perception. *Curr Dir Psychol Sci* 5:44–53
- Lu ZL, Sperling G (2001) Three-systems theory of human visual motion perception: review and update. *J Opt Soc Am A* 18:2331–2370
- Masson GS, Busetini C, Yang D-S, Miles FA (2001) Short-latency ocular following in humans: sensitivity to binocular disparity. *Vision Res* 41:3371–3387
- Masson GS, Castet E (2002) Parallel motion processing for the initiation of short-latency ocular following in humans. *J Neurosci* 22:5149–5163
- Masson GS, Rybarczyk Y, Castet E, Mestre DR (2000) Temporal dynamics of motion integration for the initiation of tracking eye movements at ultra-short latencies. *Vis Neurosci* 17:753–767
- Masson GS, Yang D-S, Miles FA (2002a) Reversed short-latency ocular following. *Vision Res* 42:2081–2087
- Masson GS, Yang D-S, Miles FA (2002b) Version and vergence eye movements in humans: open-loop dynamics determined by monocular rather than binocular image speed. *Vision Res* 42:2853–2867
- Mather G, Moulden B (1983) Thresholds for movement direction: two directions are less detectable than one. *Q J Exp Psychol A* 35:513–518
- Maunsell JH, Nealey TA, DePriest DD (1990) Magnocellular and parvocellular contributions to responses in the middle temporal visual area (MT) of the macaque monkey. *J Neurosci* 10:3323–3334

- Maunsell JH, van Essen DC (1983) The connections of the middle temporal visual area (MT) and their relationship to a cortical hierarchy in the macaque monkey. *J Neurosci* 3:2563–2586
- Merigan WH, Maunsell JH (1990) Macaque vision after magnocellular lateral geniculate lesions. *Vis Neurosci* 5:347–352
- Mikami A, Newsome WT, Wurtz RH (1986) Motion selectivity in macaque visual cortex. I. Mechanisms of direction and speed selectivity in extrastriate area MT. *J Neurophysiol* 55:1308–1327
- Miles FA (1998) The neural processing of 3-D visual information: evidence from eye movements. *Eur J Neurosci* 10:811–822
- Miles FA, Busetini C, Masson GS, Yang D-S (2004) Short-latency eye movements: evidence for rapid, parallel processing of optic flow. In: Vaina LM, Beardsley SA, Rushton S (eds) *Optic flow and beyond*. Kluwer Academic Press, Dordrecht, pp 79–107
- Miles FA, Kawano K (1986) Short-latency ocular following responses of monkey. III. Plasticity. *J Neurophysiol* 56:1381–1396
- Miles FA, Kawano K, Optican LM (1986) Short-latency ocular following responses of monkey. I. Dependence on temporospatial properties of visual input. *J Neurophysiol* 56:1321–1354
- Movshon JA, Newsome WT (1996) Visual response properties of striate cortical neurons projecting to area MT in macaque monkeys. *J Neurosci* 16:7733–7741
- Pantle A, Turano K (1992) Visual resolution of motion ambiguity with periodic luminance- and contrast-domain stimuli. *Vision Res* 32:2093–2106
- Priebe NJ, Lisberger SG, Movshon JA (2006) Tuning for spatiotemporal frequency and speed in directionally selective neurons of macaque striate cortex. *J Neurosci* 26:2941–2950
- Purpura K, Kaplan E, Shapley RM (1988) Background light and the contrast gain of primate P and M retinal ganglion cells. *Proc Natl Acad Sci USA* 85:4534–4537
- Qian N, Andersen RA (1994) Transparent motion perception as detection of unbalanced motion signals. II. Physiology. *J Neurosci* 14:7367–7380
- Qian N, Andersen RA, Adelson EH (1994) Transparent motion perception as detection of unbalanced motion signals. I. Psychophysics. *J Neurosci* 14:7357–7366
- Rodman HR, Albright TD (1987) Coding of visual stimulus velocity in area MT of the macaque. *Vision Res* 27:2035–2048
- Recanzone GH, Wurtz RH (1999) Shift in smooth pursuit initiation and MT and MST neuronal activity under different stimulus conditions. *J Neurophysiol* 82:1710–1727
- Roufs JAJ (1972a) Dynamic properties of vision. I. Experimental relationships between flicker and flash thresholds. *Vision Res* 12:261–278
- Roufs JAJ (1972b) Dynamic properties of vision. II. Theoretical relationships between flicker and flash thresholds. *Vision Res* 12:279–292
- Rust NC (2004) Signal transmission, feature representation and computation in areas V1 and MT of the macaque monkey. Doctoral dissertation, New York University, Dissertation Abstracts International 65/09-B, 4444
- Rust NC, Mante V, Simoncelli EP, Movshon JA (2006) How MT cells analyze the motion of visual patterns. *Nat Neurosci* 9:1421–1431
- Rust NC, Schwartz O, Movshon JA, Simoncelli EP (2005) Spatiotemporal elements of macaque v1 receptive fields. *Neuron* 46:945–956
- Saito H, Yukie M, Tanaka K, Hikosaka K, Fukada Y, Iwai E (1986) Integration of direction signals of image motion in the superior temporal sulcus of the macaque monkey. *J Neurosci* 6:145–157
- Schiller PH, Logothetis NK, Charles ER (1990) Role of the color-opponent and broad-band channels in vision. *Vis Neurosci* 5:321–346
- Sheliga BM, Chen KJ, FitzGibbon EJ, Miles FA (2005a) Initial ocular following in humans: a response to first-order motion energy. *Vision Res* 45:3307–3321
- Sheliga BM, Chen KJ, FitzGibbon EJ, Miles FA (2005b) Short-latency disparity vergence in humans: evidence for early spatial filtering. *Ann NY Acad Sci* 1039:252–259
- Sheliga BM, Chen KJ, FitzGibbon EJ, Miles FA (2006a) The initial ocular following responses elicited by apparent-motion stimuli: Reversal by inter-stimulus intervals. *Vision Res* 46:979–992

- Sheliga BM, FitzGibbon EJ, Miles FA (2006b) Short-latency disparity vergence eye movements: a response to disparity energy. *Vision Res* 46:3723–3740
- Sheliga BM, FitzGibbon EJ, Miles FA (2007a) Competing image motions: evidence for local and global nonlinear interactions. 2007 Neuroscience Meeting Planner. Program No. 337.314. Society for Neuroscience, San Diego, CA
- Sheliga BM, FitzGibbon EJ, Miles FA (2007b) Human vergence eye movements initiated by competing disparities: evidence for a winner-take-all mechanism. *Vision Res* 47:479–500
- Sheliga BM, FitzGibbon EJ, Miles FA (2008) Human ocular following: evidence that responses to large-field stimuli are limited by local and global inhibitory influences. *Prog Brain Res* 171:237–243
- Sheliga BM, Kodaka Y, FitzGibbon EJ, Miles FA (2006c) Human ocular following initiated by competing image motions: evidence for a winner-take-all mechanism. *Vision Res* 46:2041–2060
- Shioiri S, Cavanagh P (1990) ISI produces reverse apparent motion. *Vision Res* 30:757–768
- Simoncelli EP, Heeger DJ (1998) A model of neuronal responses in visual area MT. *Vision Res* 38:743–761
- Smith AT (1994) Correspondence-based and energy-based detection of second-order motion in human vision. *J Opt Soc Am A* 11:1940–1948
- Snowden RJ, Hess RF, Waugh SJ (1995) The processing of temporal modulation at different levels of retinal illuminance. *Vision Res* 35:775–789
- Snowden RJ, Treue S, Erickson RG, Andersen RA (1991) The response of area MT and V1 neurons to transparent motion. *J Neurosci* 11:2768–2785
- Stromeyer CF, Kronauer RE, Madsen JC, Klein SA (1984) Opponent-movement mechanisms in human vision. *J Opt Soc Am A* 1:876–884
- Strout JJ, Pantle A, Mills SL (1994) An energy model of interframe interval effects in single-step apparent motion. *Vision Res* 34:3223–3240
- Swanson WH, Ueno T, Smith VC, Pokorny J (1987) Temporal modulation sensitivity and pulse-detection thresholds for chromatic and luminance perturbations. *J Opt Soc Am A* 4:1992–2005
- Takemura A, Inoue Y, Kawano K (2000) The effect of disparity on the very earliest ocular following responses and the initial neuronal activity in monkey cortical area MST. *Neurosci Res* 38:93–101
- Takemura A, Inoue Y, Kawano K (2002) Visually driven eye movements elicited at ultra-short latency are severely impaired by MST lesions. *Ann N Y Acad Sci* 956:456–459
- Takemura A, Kawano K (2002) Sensory-to-motor processing of the ocular-following response. *Neurosci Res* 43:201–206
- Takemura A, Kawano K (2006) Neuronal responses in MST reflect the post-saccadic enhancement of short-latency ocular following responses. *Exp Brain Res* 173:174–179
- Takemura A, Murata Y, Kawano K, Miles FA (2007) Deficits in short-latency tracking eye movements after chemical lesions in monkey cortical areas MT and MST. *J Neurosci* 27:529–541
- Takeuchi T, De Valois KK (1997) Motion-reversal reveals two motion mechanisms functioning in scotopic vision. *Vision Res* 37:745–755
- Takeuchi T, De Valois KK, Motoyoshi I (2001) Light adaptation in motion direction judgments. *J Opt Soc Am A* 18:755–764
- Tanaka K, Hikosaka K, Saito H, Yukie M, Fukada Y, Iwai E (1986) Analysis of local and wide-field movements in the superior temporal visual areas of the macaque monkey. *J Neurosci* 6:134–144
- Tanaka K, Saito H (1989) Analysis of motion of the visual field by direction, expansion/contraction, and rotation cells clustered in the dorsal part of the medial superior temporal area of the macaque monkey. *J Neurophysiol* 62:626–641
- Ungerleider LG, Desimone R (1986) Cortical connections of visual area MT in the macaque. *J Comp Neurol* 248:190–222
- van Santen JP, Sperling G (1984) Temporal covariance model of human motion perception. *J Opt Soc Am A* 1:451–473

- van Santen JP, Sperling G (1985) Elaborated Reichardt detectors. *J Opt Soc Am A* 2:300–321
- Watson AB, Ahumada AJ (1985) Model of human visual-motion sensing. *J Opt Soc Am A* 2:322–341
- Wurtz RH (1998) Optic flow: a brain region devoted to optic flow analysis? *Curr Biol* 8:R554–R556
- Yang D-S, FitzGibbon EJ, Miles FA (1999) Short-latency vergence eye movements induced by radial optic flow in humans: dependence on ambient vergence level. *J Neurophysiol* 81:945–949
- Yang D-S, FitzGibbon EJ, Miles FA (2003) Short-latency disparity-vergence eye movements in humans: sensitivity to simulated orthogonal tropias. *Vision Res* 43:431–443
- Yang D-S, Miles FA (2003) Short-latency ocular following in humans is dependent on absolute (rather than relative) binocular disparity. *Vision Res* 43:1387–1396
- Zemany L, Stromeyer CF, Chaparro A, Kronauer RE (1998) Motion detection on flashed, stationary pedestal gratings: evidence for an opponent-motion mechanism. *Vision Res* 38:795–812